A Model of PSI Dimerization: Destabilization of the $C^{278}-G^{303}$ Stem−Loop by the Nucleocapsid Protein (NCp10) of MoMuLV†

Pierre-Marie Girard,‡,§ Hugues de Rocquigny,|| Bernard-Pierre Roques,|| and Jacques Paoletti*,‡

Unité de Biochimie, URA 147 CNRS, 39 rue Camille Desmoulins, Institut Gustave Roussy, 94805 Villejuif, France, and Département de Pharmacochimie Moléculaire et Structurale, INSERM U266-URA, D1500 CNRS, Faculté de Pharmacie, Université René Descartes, 4, Avenue de l'Observatoire, 75270 Paris Cedex 06, France

Received October 16, 1995; Revised Manuscript Received April 9, 1996⊗

ABSTRACT: We have shown that at low ionic strength (i.e., 100 mM NaCl) a short autocomplementary sequence spanning nucleotides C^{283} to G^{298} of MoMuLV RNA genome is involved in the process of PSI dimerization *in vitro* [Girard, P.-M., Bonnet-Mathonière, B., Muriaux, D., & Paoletti, J. (1995) *Biochemistry 34,* 9785−9794]. In order to identify other contributions of the PSI structure to RNA dimerization, we studied the kinetics of dimerization as a function of salt concentration of short RNA transcripts comprising or not the autocomplementary sequence $C^{283}-G^{298}$. We propose that, apart from the crucial role of this sequence in RNA dimerization, the 364−565 domain of PSI can interfere, *in vitro*, with the initiation of dimer formation. Intermolecular loop−loop recognitions involving the 364−565 domain could stabilize, in a salt concentration-dependent manner, a transient RNA dimer built around the loop−loop $U^{288}-A^{293}$ interaction. This dimer evolves toward a more stable structure which mainly corresponds to the annealing of two $C^{283}-G^{298}$ sequences. We also show that chemically synthesized NCp10 does not modify these steps but rather helps the system to pass over the energy barriers associated with the transition to stable RNA structures comprising the stem−loop $C^{278}-G^{303}$. Data obtained in the presence of NCp10 suggest a binding site size of 9 ± 1 nucleotides per protein at 37 °C and a 10−20-fold increase in the rate constant (i.e., $k_1 = 24\,000 \pm 7000\ M^{-1}\ s^{-1}$) of dimer formation.

The 60−70S RNA extracted from MoMuLV[1] retroviral particles results from noncovalent association of two identical 30−35S genomic RNAs of 8332 nts. As shown by electron microscopy studies, the region of interaction that was named DLS (Bender & Davidson, 1976) involves sequences and/or structures localized near the 5′-terminal noncoding region of each genomic RNA (Hu et al., 1977; Maisel et al., 1978; Bender et al., 1978; Murti et al., 1981). In the experimental conditions (i.e., urea and formamide as denaturing agents) the DLS corresponds to the strongest region of stability and could involve less than 50 nts (Murti et al., 1981). The DLS was localized inside a short sequence ranging from nts 215 to 565, referred to as PSI, that is necessary for efficient retroviral RNA encapsidation [Mann et al., 1983; Mann & Baltimore, 1985; for review see Rein (1994)]. *In vitro*, PSI is able to dimerize in the absence of trans-acting factor in a salt concentration-, RNA concentration-, and temperature-dependent manner (Roy et al., 1990).

We have shown that *in vitro* dimerization of short RNA transcripts corresponding to the 5′-terminal noncoding region of MoMuLV RNA genome involved a nearly perfect autocomplementary sequence spanning nucleotides C^{278} to G^{303} that can adopt a stem−loop structure (Tounekti et al., 1992; Girard et al., 1995). The overall dimerization process of MoMuLV RNA transcripts can be described in at least three steps: (1) a temperature-dependent intramolecular process ($M \rightarrow M^*$) leading to a "dimerizable" conformation of the RNA monomer, (2) a loop−loop recognition through the $U^{288}AGCUA^{293}$ sequence leading to an unstable dimer ($M^* + M^* \leftrightarrow D1$), and (3) the evolution of D1 toward a stable dimer D2 ($D1 \rightarrow D2$). Could this region be the only structural feature implicated in RNA−RNA interaction, or do regions located upstream and downstream the $C^{283}-G^{298}$ sequence contribute to the overall process of dimerization?

Inside the retroviral capsid, genomic RNA is in close association with a large number of nucleocapsid proteins (NCp) (Fleissner & Tress, 1973; Darlix & Spahr, 1982). Retroviral NCp are small, basic nucleic acid binding polypeptides highly conserved within retroviruses (Long et al., 1980; Covey, 1986; Leis et al., 1988). NCp are thought to stabilize the dimeric RNA genome through formation of a ribonucleoprotein complex (Nissen-Meyer & Abraham, 1980; Darlix et al., 1990) that ensures its protection from nucleases (Aronoff et al., 1993). All retroviral NCp sequenced so far, excluding the human spumaretrovirus (Maurer et al., 1988), contain either one (e.g., MoMuLV) or two copies (e.g., HIV and RSV) of the conserved sequence Cys-aa_2-Cys-aa_4-His-aa_4-Cys referred to as the cysteine−histidine

† This work was supported by the Agence Nationale de la Recherche sur le SIDA (ANRS).

* To whom correspondence should be addressed.

‡ Unité de Biochimie, URA 147 CNRS.

§ Present address: Oncogénèse Appliquée, INSERM U268, Hôpital Paul Brousse, 14, Avenue Paul Vaillant Couturier, 94800 Villejuif, France.

|| Département de Pharmacochimie Moléculaire et Structurale, INSERM U266-URA.

⊗ Abstract published in *Advance ACS Abstracts,* June 1, 1996.

[1] Abbreviations: aa, amino acid; DLS, dimer linkage structure; DTT, dithiothreitol; EDTA, ethylendiaminetetraacetic acid; EGTA, ethylene glycol bis(β-aminoethyl ether) *N,N,N′,N′*-tetraacetic acid; HIV, human immunodeficiency virus; MoMuLV, Moloney murine leukemia virus; MW, molecular weight; NCp, nucleocapsid protein; NMR, nuclear magnetic resonance; nt(s), nucleotide(s); RSV, Rous sarcoma virus; SDS, sodium dodecyl sulfate; TBE, Tris−borate−EDTA; TFA, trifluoroacetic acid; T_M, melting temperature.

S0006-2960(95)02454-8 CCC: $12.00

or CCHC box (Méric & Spahr, 1986) that bind a zinc atom with very high affinity, $K_a \gg 10^{13}$ M^{-1} (Cornille et al., 1990; Mély et al., 1991). The ^{1}H NMR structures of the MoMuLV NCp10 (Déméné et al., 1994a) and of the HIV-1 NCp7 (Morellet et al., 1992, 1994; Omichinski et al., 1991) have shown that the zinc atom is tetracoordinated to the CCHC residues, resulting in well-defined folded zinc finger domains. Point mutations of the conserved Cys and His residues result in a drastic reduction of genomic RNA packaging (Méric et al., 1988; Gorelick et al., 1988, 1990; Bowles et al., 1993; Dorfman et al., 1993; Déméné et al., 1994b; Morellet et al., 1994; Rein et al., 1994). Darlix and co-workers have also suggested that NCp could (1) activate viral RNA transcript dimerization (Prats et al., 1988, 1990, 1991; Bieth et al., 1990; Darlix et al., 1990; de Rocquigny et al., 1992), (2) promote the annealing of primer tRNAs to the primer binding site (PBS), an essential step for the initiation of reverse transcription (Barat et al., 1989, 1993; Darlix et al., 1992; de Rocquigny et al., 1992; Lapadat-Tapolsky et al., 1993), (3) favor the minus strand DNA transfer during reverse transcription (Lapadat-Tapolsky et al., 1993; Allain et al., 1994), and (4) slightly stimulate the cleavage reaction catalyzed by integrase, suggesting a possible involvement of NCp in provirus integration (Lapadat-Tapolsky et al., 1993).

In this work, we investigated the *in vitro* dimerization of MoMuLV RNA transcripts in the presence or absence of solid-phase synthesized NCp10. We propose a model of PSI RNA dimerization that takes into account the overall RNA structure. In this model, we suggest that stem−loop structures localized in the 364−565 domain of PSI RNA favor the process of dimerization through complementary loop−loop recognitions. We also report that in the presence of NCp10 the autocomplementary sequence C^{283}−G^{298} is mainly involved in RNA dimer formation and in the thermal stability of RNA dimers, suggesting that this sequence could be all or part of the dimer linkage structure (DLS).

MATERIALS AND METHODS

Plasmid Construction and Digestion for in Vitro Transcription. Standard procedures were used for restriction enzyme digestion and plasmid construction (Sambrook et al., 1989). *Escherichia coli* DH5α was used for plasmid amplification.

RNA transcripts f215−565 (380 nts in length), f215−364 (172 nts in length), and f215−282 (93 nts in length) were prepared as previously described (Girard et al., 1995).

For RNA transcripts f215−565Δ279−302 (361 nts in length) and f215−364Δ279−302 (153 nts in length), polymerase chain reaction was performed on pCR2 (Roy et al., 1990) with two sets of oligonucleotides: the first set contained oligonucleotide AVA278−262 (5′CTCGGGACGCAGGCGCATAAAA3′), carrying an *Ava*I site and 17 nucleotides corresponding to the complementary part of positions +278 to +262 of the MoMuLV RNA genome, and M13 universal primer. The second set contained oligonucleotide AVA303−319 (5′CCCGAGTATCTGGCGGACCCGT3′), which corresponds to positions +303 to +319 of the MoMuLV genome and carries an *Ava*I site, and T3 universal primer. The amplified products were purified, digested with *Ava*I, and ligated to each other. The DNA fragments obtained, which lack nucleotides 279−302 of the MoMuLV genome, were digested with *Eco*RI and *Hin*dIII and ligated into the *Eco*RI and *Hin*dIII sites of pGEM3ZF(−), thus generating p215−565Δ279−302. After linearization at the *Hin*dIII or *Bsa*HI sites, this plasmid was transcribed with T7 RNA polymerase, giving rise to f215−565Δ279−302 or f215−364Δ279−302, respectively. Due to the construction, the same non-MoMuLV sequence as described for RNA transcript 215−565 is present at the 5′ end of these transcripts (Girard et al., 1995; see also Figure 1).

For RNA transcripts f283−364 (89 nts in length), pCR2 (Roy et al., 1990) was linearized with the restriction endonuclease *Spe*I and end-filled using the Klenow fragment of DNA polymerase I (New England Biolabs). The reactions were phenol-extracted, and after ethanol precipitation, the DNA was digested by the restriction endonuclease *Pst*I, resulting in two DNA fragments. The 285 bp DNA fragment was purified and ligated between the *Eco*RI site that was blunt-ended using S1 nuclease and the *Pst*I site of pGEM3ZF(−), thus generating p283−565. After linearization at the *Bsa*HI site, the plasmid was transcribed with T7 RNA polymerase, giving rise to transcripts starting at position 283 of MoMuLV RNA sequence and ending at position 364. These fragments are referred to as f283−364. The five non-MoMuLV nucleotides (GGGCG) are present at the 5′ end of these transcripts (Figure 1).

RNA Synthesis and Purification. Experimental conditions used for *in vitro* transcription and purification are described by Girard et al. (1995). The purity and integrity of RNA transcripts were checked by polyacrylamide gel electrophoresis in denaturing conditions, and the RNA strand concentration was determinated by UV spectroscopic measurement at 260 nm.

In Vitro Dimerization without NCp10. Kinetics of dimerization were achieved as described by Girard et al. (1995) with a 5-fold concentrated buffer leading to 50 mM Tris-HCl, pH 7, and 50−700 mM NaCl in final concentration. The samples were incubated for 0−120 min at 50 °C. At the end of incubation, all the samples were cooled on ice, mixed with 2 μL of loading buffer (50% w/v glycerol and 0.025% w/v tracking dyes), loaded on 1.5% (w/v) Seakem−0.5% (w/v) Nusieve agarose gel, and electrophoresed at 5 V/cm at 4 °C, in buffer containing 50 mM Tris−borate, pH 8.3, 1 mM EDTA, and 0.2 μg/mL ethidium bromide. Oligonucleotide inhibition was as described by Girard et al. (1995) in buffer D_{250} (250 mM NaCl, 50 mM Tris-HCl, pH 7).

MoMuLV NCp10. Solid-phase synthesis of the retroviral nucleocapsid protein NCp10 (56 aa, MW = 6362) was performed using the Fmoc procedure with DCC/HOBt as coupling reagents on a HMP resin (de Rocquigny et al., 1993). Assembly of the protected peptide chains was carried out using the stepwise solid-phase method of Merrifield (Barany & Merrifield, 1979) on an ABI 431A (Perkin-Elmer). Amino acid analysis and NH_2-terminal sequencing were performed on a System 6300 Beckman apparatus (Palo Alto, CA) and on a Model 477A Applied Biosystems sequencer, respectively. The SH content of NCp10 was checked by titration at 412 nm with 5,5′-dithiobis(2-nitrobenzoic acid) as already described (de Rocquigny et al., 1993) and suggested that more than 90% of the SH groups were in a reduced state. Considering the molar extinction coefficient of 7000 M^{-1} cm^{-1} at 280 nm (Cornille et al., 1990), stock solution of NCp10 was prepared at 1.24×10^{-3} M in Milli-Q (Millipore) water, and an equivalent molar

concentration of $ZnSO_4$ was added.

The various NCp10/RNA molecular ratios (r) were prepared as follows: a concentrated solution (in referring to RNA strand concentration) of NCp10 was prepared from a stock solution of NCp10 in a 40 μL final volume of buffer NCp (buffer NCp = 20 mM Tris-HCl, pH 7.5, 50 mM NaCl, 0.2 mM $MgCl_2$, and 5 mM DTT) and by adding 1 μL of RNasin (RNase inhibitor, Promega). Subsequent dilutions of 10-fold concentrated solutions of NCp10 were prepared from this one in buffer NCp and were then kept for 15 min at room temperature prior to RNA addition, as described below.

MoMuLV RNA Transcript Dimerization in the Presence of NCp10. In a standard dimerization assay, RNA, in 21 μL of Milli-Q water, was heated for 2 min at 90 °C, chilled on ice for 2 min, and adjusted to 30 μL with 6 μL of 5-fold concentrated buffer NCp and 3 μL of 10-fold concentrated NCp10 (or 3 μL of Milli-Q water). The samples were incubated for 15 min at temperatures ranging from 4 to 50 °C. For kinetics of dimerization, samples were incubated at 37 °C for an incubation time varying from 0 to 60 min. After incubation, all the samples were cooled on ice for 2 min, placed for 2 min at room temperature, and then mixed with 3 μL of 5% SDS for another 5 min at room temperature. Forty microliters of phenol saturated by 40 mM Tris-HCl, pH 6.5, 0.1% SDS, and 2.5 mM EGTA was added, and the samples were mixed vigorously. Six microliters of loading buffer (50% w/v glycerol and 0.025% w/v tracking dyes) was then added to 30 μL of the upper phase, and the samples were loaded on 1.5% (w/v) Seakem−0.5% (w/v) Nusieve agarose gel and electrophoresed at 5 V/cm and 4 °C, in buffer containing 50 mM Tris−borate, pH 8.3, 1 mM EDTA, and 0.2 μg/mL ethidium bromide.

Monomer and Dimer Determination. Gels were scanned for fluorescence by a Bioprofil apparatus (Vilber-Lourmat, France), and peak surface corresponding to dimer (PS_{dimer}) and monomer ($PS_{monomer}$) species was integrated. Assuming that the sensitivity of ethidium bromide toward monomer and dimer is the same and that the fluorescence intensity of each band only depends on RNA concentration, the amount of dimer obtained at each incubation time (D_{time}) was then calculated by applying the following relation: $(D_{time}) = (PS_{dimer})/(PS_{dimer} + PS_{monomer})$. The rate constant of the reaction (k_1) and the total amount of dimer (D_{tot}) were derived by assuming a simple bimolecular reaction and solving the integrated form of the equation.

RESULTS

Oligonucleotide Inhibition. RNA dimer formation of short transcripts corresponding to the 5′-terminal noncoding region of the MoMuLV RNA genome (Figure 1) is a slow process, which implies conformational rearrangements of both monomeric and dimeric RNA (Roy et al., 1990; Girard et al., 1995). A major structural feature of this process is the involvement of a short autocomplementary sequence (nucleotides 283 to 298) at low ionic strength (i.e., buffer D_{100} = 50 mM Tris-HCl, pH 7, 100 mM NaCl). Oligonucleotide OL275−291, which is complementary to nucleotides 275−291 of the MoMuLV RNA genome, inhibited at 90% f215−565 (also called RNA PSI) and f215−364 dimerization in buffer D_{100} and at 50 °C at an oligonucleotide/RNA ratio of 5/1 (Girard et al., 1995). Similar experiments conducted in buffer D_{250} (50 mM Tris-HCl, pH 7, 250 mM NaCl) revealed

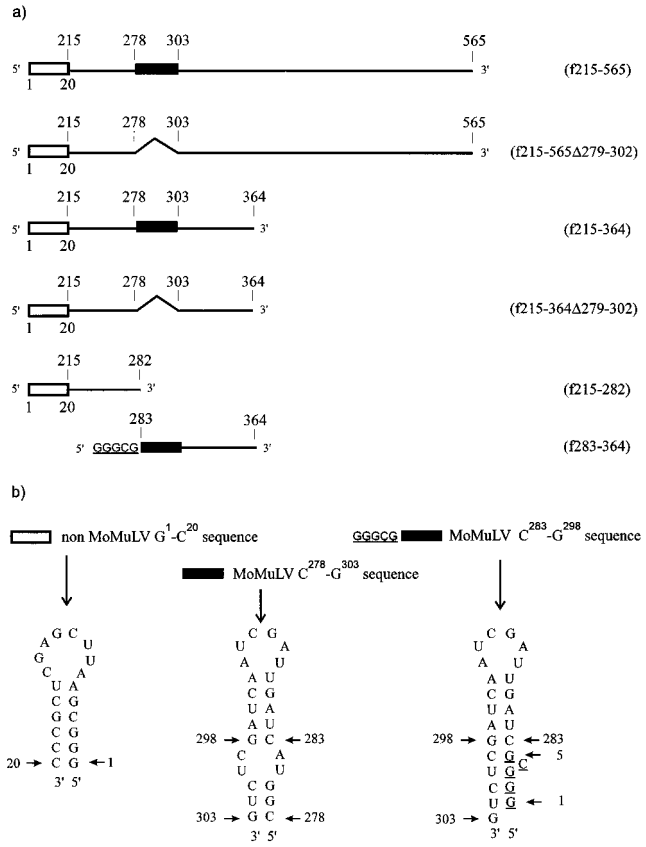

FIGURE 1: Mapping of the sequence necessary for MoMuLV RNA dimerization. (a) MoMuLV RNA transcripts used in this study. Numbering from 215 to 565 is in relation to the cap site (+1) of the MoMuLV RNA genome. Note that non-MoMuLV sequences are present at the 5′ end of these transcripts (numbering from 1 to 20 and GGGCG sequence). △ symbolizes a deletion from nucleotides 278 to 303. Opened and filled rectangles characterize two nearly perfect autocomplementary sequences. (b) Predictive secondary structure of these sequences at 37 °C determined by MFOLD software (Zuker, 1989a,b).

that dimerization of f215−565 is not inhibited by OL275−291 even at an oligonucleotide/RNA ratio of 5/1 whereas f215−364 RNA is 90% inhibited (Figure 2). This suggests that at 250 mM NaCl f215−364 dimer formation should be centered on the 278−303 sequence while nucleotides downstream of nt 364 are involved in f215−565 dimer formation either through a self-association or an interaction with the 215−364 region.

Kinetics of Dimerization as a Function of NaCl Concentration. The contribution of RNA structure to dimer formation was assayed by following the kinetics of dimerization of short RNA transcripts at 50 °C as a function of salt concentration (from 50 to 700 mM NaCl). The proportion of dimer (D_{tot}) and the rate constant (k_1) were derived, as described in Materials and Methods, and plotted as shown in Figure 3. From 50 to 250 mM NaCl, k_1 of f215−565 dimerization linearly increases 25-fold with a slope (d log [k_1]/d log [NaCl]) of 2.2 ± 0.4 and decreases from 400 mM NaCl (Figure 3b). As shown in Figure 3a, this diminution was not correlated with a low dimerization yield as D_{tot} was 100% at NaCl concentrations ≥100 mM. On the other hand, k_1 for f215−364 dimerization increased linearly between 50 and 700 mM NaCl (Figure 3b) with a d log [k_1]/d log [NaCl] slope of 0.9 ± 0.2 and k_1 values 3−23 times lower than those of f215−565 dimerization between 50 and 250 mM NaCl. In addition, less than 15% of f215−282 dimer (RNA transcript lacking the entire autocomplementary sequence;

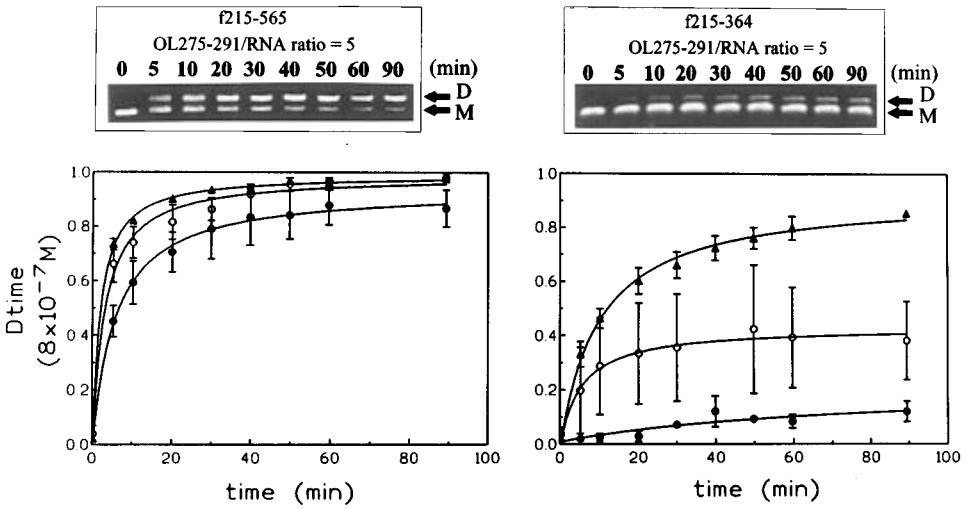

FIGURE 2: Kinetics of f215−565 and f215−364 dimerization in buffer D_{250} at 50 °C without (▲) or with oligonucleotide OL275−291 at an oligonucleotide/RNA ratio of 1/1 (○) or 5/1 (●). (Up) Ethidium bromide stained agarose gel electrophoresis at an oligonucleotide/RNA ratio of 5/1. M and D indicate monomeric and dimeric RNA species, respectively. (Down) Representation of the relative percent of RNA dimer as a function of time. Gels were scanned for fluorescence, and the concentration of each RNA species was calculated (see Materials and Methods). The total RNA strand concentration is 0.8 μM.

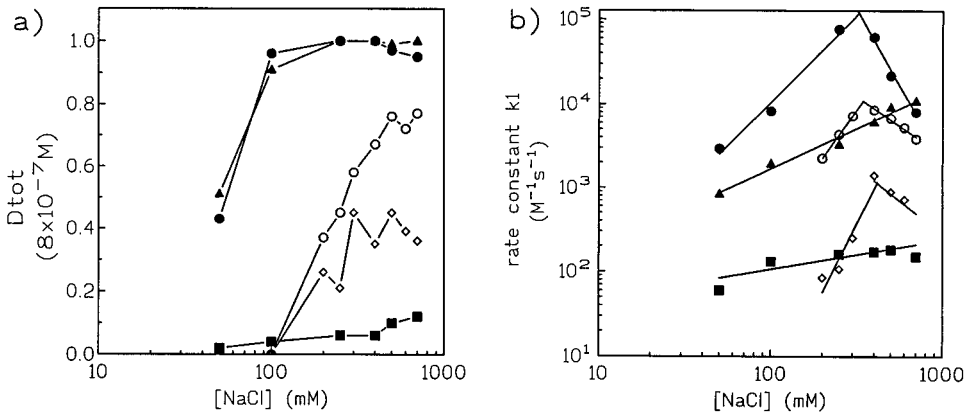

FIGURE 3: Representation of (a) the total amount of dimer (D_{tot}) and (b) the rate constant k_1 as a function of salt concentration for f215−565 (●), f215−364 (▲), f215−565Δ279−302 (○), f215−364Δ279−302 (◇), and f215−282 (■). △ symbolizes a deletion of nts 279−302. These data were derived from kinetics of dimerization performed in 50 mM Tris-HCl, pH 7, and NaCl concentration ranging from 50 to 700 mM assuming a simple bimolecular reaction (M + M ↔ D). The total RNA strand concentration is 0.8 μM.

see Figure 1) is observed below 700 mM NaCl (Figure 3a) with rate constants varying between 10^2 and 2×10^2 M^{-1} s^{-1} (Figure 3b). These results, together with the inhibition induced by the OL275−291 antisense oligonucleotide, support the idea that the dimerization of the 215−364 region is triggered by the sequence spanning nt 278 to 303 and that the 364−565 region could increase the kinetics of dimerization.

To ascertain the role of the 364−565 domain in dimerization, RNAs f215−565 or f215−364 bearing a deletion of nts 279 to 302 (f215−565Δ279−302 and f215−364Δ279−302, respectively) were tested at 50 °C for their ability to dimerize in 50 mM Tris-HCl, pH 7, and 50−700 mM NaCl. Figure 3a shows that these transcripts do not significantly dimerize at NaCl concentrations ≤100 mM and are ≥30% dimeric at NaCl concentrations ≥300 mM. The deletion lowers k_1 values by 1 order of magnitude (Figure 3b). This suggests a contribution of at least three regions in the dimerization process: stem−loop C^{278}−G^{303}, all or part of the 364−565 region, and the 303−364 region. In our experimental conditions, the autocomplementary sequence C^{283}−G^{298} is required for a wild-type dimer yield at all salt concentrations whereas the 364−565 domain only increases the kinetics of dimerization.

Kinetics of f215−565 and f215−565Δ279−302 Dimerization at 37 °C as a Function of NCp10 Concentration. Darlix and co-workers have shown that NCp10 favors RNA dimer formation *in vitro* at low ionic strength (Bieth et al., 1990; Prats et al., 1988, 1990, 1991; Darlix et al., 1990; de Rocquigny et al., 1993). Thus, it was of interest to determine which part of the PSI RNA structure is responsible for RNA dimer formation triggered by the NCp10. For this purpose, kinetics of f215−565 and f215−565Δ279−302 dimerization were performed at physiological temperature (37 °C) in NCp 1× buffer (20 mM Tris-HCl, pH 7.5, 50 mM NaCl, 0.2 mM $MgCl_2$, and 5 mM DTT) with increasing NCp10/RNA molecular ratio ranging from $r = 0$ to $r = 100$ (i.e., until 3−4 nts per NCp10). The proteins were removed by phenol−SDS extraction and the samples analyzed on 2% agarose gels (Figure 4). The total amount of dimer (D_{tot}) and rate constant (k_1) were derived as already described in Materials and Methods. The D_{tot} of f215−565 reached 100% after a 60 min incubation at 37 °C in the presence of 100 NCp10/RNA (Figure 4a) that corresponds to around 3.8 nts per NCp10. In contrast, the D_{tot} of f215−565Δ279−302 was ≤40% and was independent of NCp10 concentration (Figure 4b). Furthermore, the plot of the logarithm of k_1 as a function of NCp10 concentration leads to a curve with f215−565 that

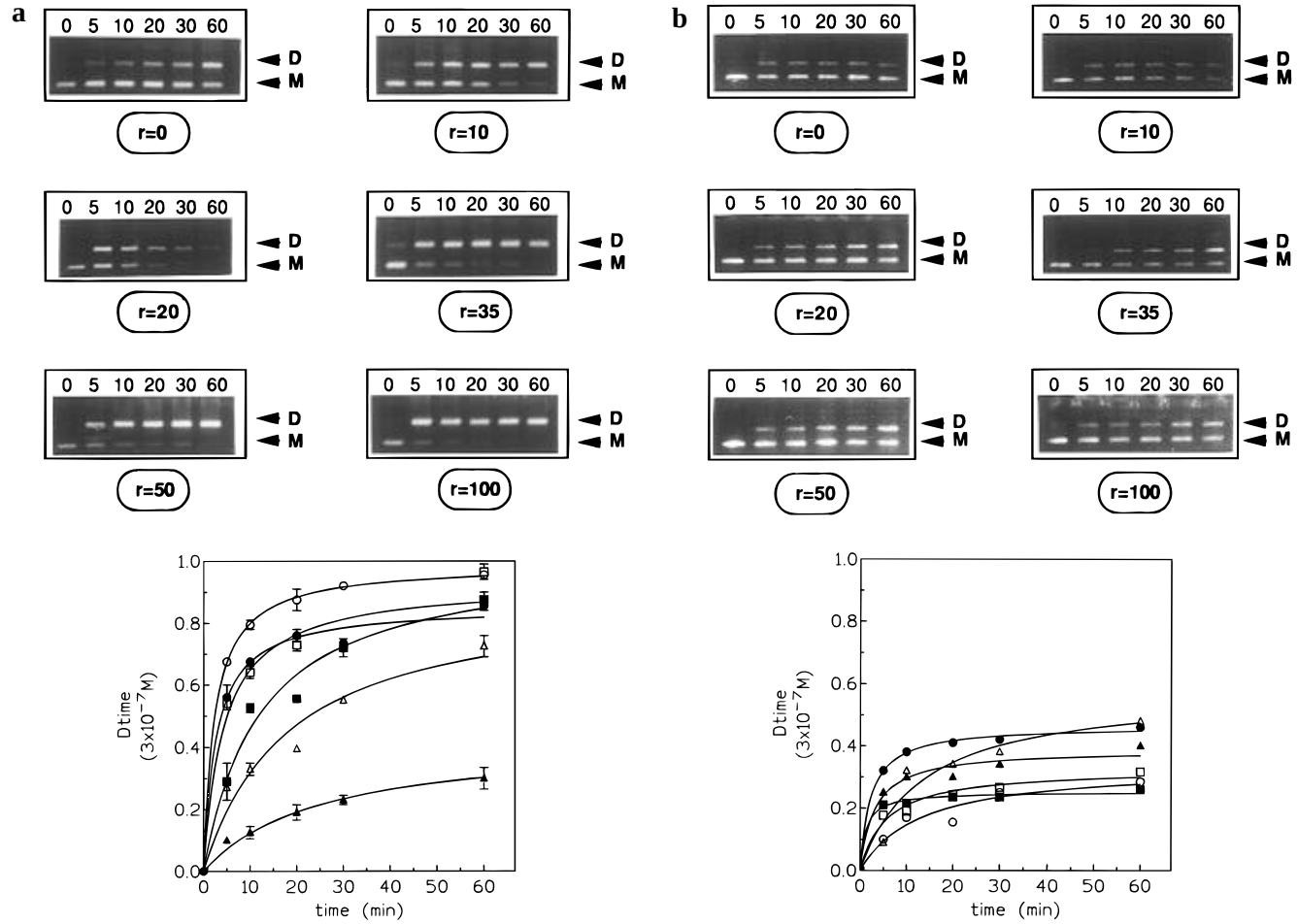

FIGURE 4: Kinetics of dimerization of f215−565 (a) and f215−565Δ279−302 (b) as a function of NCp10 concentation in 30 μL of 20 mM Tris-HCl, pH 7.5, 50 mM NaCl, 0.2 mM $MgCl_2$, and 5 mM DTT (buffer NCp 1×) at 37 °C for a total RNA strand concentration of 0.3 μM. (Up) Ethidium bromide stained agarose gel electrophoresis. *r* corresponds to the NCp10/RNA molecular ratio. Time (0 to 60) is expressed in minutes. M and D correspond to monomer and dimer species, respectively. (Down) Representation of the amount of dimer (D_{time}) as a function of time at various NCp10/RNA ratios ranging between $r = 0$ (▲), $r = 10$ (≈36−38 nts per NCp10) (△), $r = 20$ (≈18−19 nts per NCp10) (■), $r = 35$ (≈10−11 nts per NCp10) (□), $r = 50$ (≈7−8 nts per NCp10) (●), and $r = 100$ (≈3−4 nts per NCp10) (○).

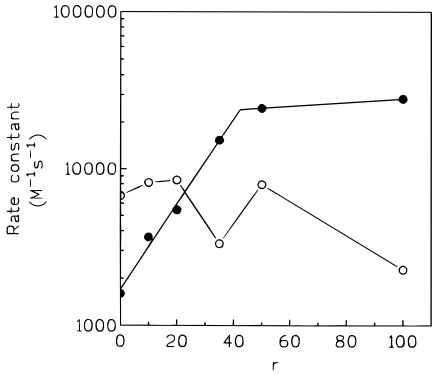

FIGURE 5: Representation of the rate constant k_1 as a function of NCp10/RNA ratio. These k_1 values were derived from kinetics of f215−565 (380 nt in length) (●) and of f215−565Δ279−302 (361 nts in length) (○) shown in Figure 4. Considering f215−565, k_1 evolves from 1600 ± 160 to 15300 ± 5700 M^{-1} s^{-1} between $r = 0$ and $r = 35$.

increases linearly to reach a plateau whereas NCp10 does not favor the dimerization process of f215−565Δ279−302 (Figure 5). These results suggest that NCp10 enhances the dimerization process if the $C^{278}-G^{303}$ domain takes part in the overall process. Then, considering f215−565 dimerization (Figure 5), the most efficient stoichiometry is determined to be around 40−45 NCp10 per RNA molecule. This corresponds to a theoretical binding site size of 9 ± 1 nucleotides per NCp10 and a rate constant of 24 000 ± 7000 M^{-1} s^{-1}. Taking into account these data, f215−565 dimer formation was enhanced 10−20-fold upon addition of chemically synthesized NCp10.

NCp10 Annealing Activity as a Function of Temperature. We have already described a three-step dimerization process of MoMuLV RNA transcripts *in vitro* which is dependent upon temperature (Girard et al., 1995). Consequently, we tried to determine how this process is modified in the presence of NCp10. For this purpose, f215−565 dimerization was followed between 4 and 50 °C in NCp 1× buffer at various incubation times and in the presence of increasing concentrations of NCp10 (Figure 6). For temperature higher than 30 °C and for $r = 50$ (corresponding to 7−8 nts per NCp10) more than 90% of f215−565 RNA molecules were dimeric after 15 min of incubation, suggesting that NCp10 increases the kinetics of PSI dimer formation in this range of temperature (Figure 6a). At $r > 75$ (i.e., <5 nts per NCp10), high molecular weight RNA/RNA and/or protein/RNA complexes are formed as observed by the presence of fluorescence at the top of the wells. For temperatures <30 °C, dimerization was incomplete even at $r = 150$ (i.e., at 2−3 nts per NCp10) (Figure 6a). To better understand if this incomplete dimerization is due rather to an insufficient incubation time and/or a nondimerizable conformation of PSI RNA at these temperatures (Girard et al., 1995), f215−565

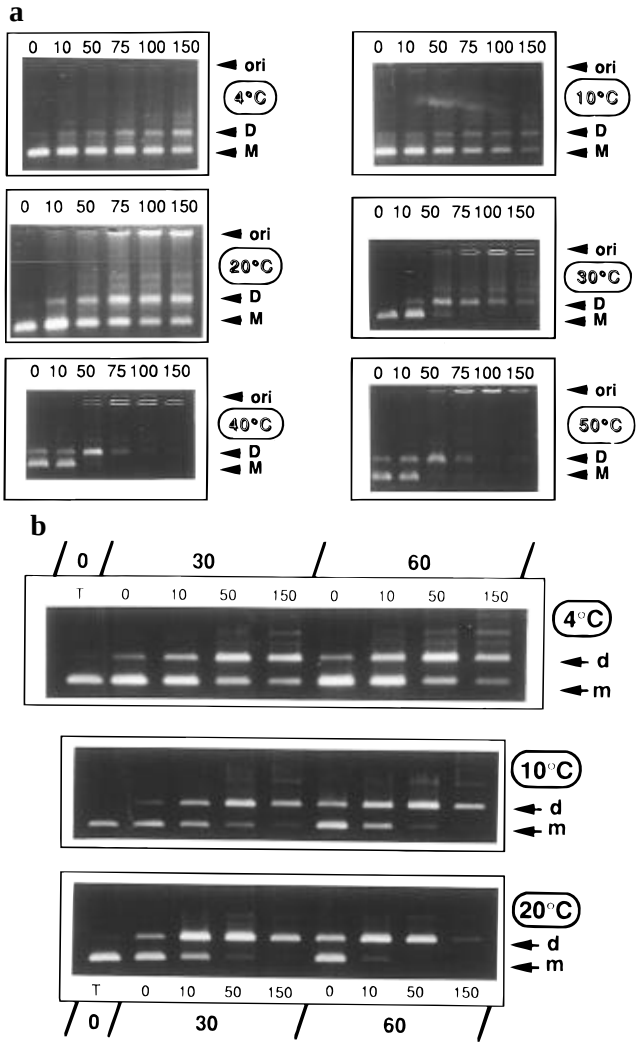

FIGURE 6: Agarose gel electrophoresis of f215−565 dimerization in the presence of different NCp10/RNA molecular ratios (*r*) between 0 and 150 and at temperatures ranging from 4 to 50 °C. Dimer formation after an incubation time of 15 min (a) or until 60 min (b). The column denoted *T* is a control. Experiments were performed in buffer NCp, and the proteins were phenol extracted as described in Materials and Methods prior to loading. M and D correspond to monomer and dimer species, respectively, and ori designs the wells.

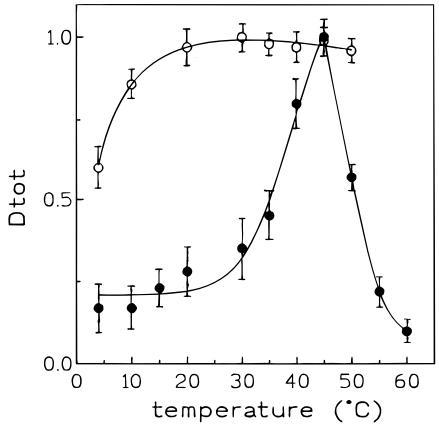

FIGURE 7: Representation of the total amount of f215−565 dimer (D_{tot}) as a function of temperature. These data were derived from kinetics undertaken in the presence of NCp10 (○) (the related experiments are shown in Figure 6) or without NCp10 (●) in buffer NCp 1×.

was incubated at temperatures <30 °C for at least 60 min. In these conditions, most of the RNA molecules were dimeric from $r = 50$ (i.e., at 7−8 nts per NCp10) (Figure 6b). The D_{tot} values derived from Figure 6 as well as those obtained from kinetics of f215−565 dimerization conducted without NCp10 (data not shown) were reported in Figure 7. Such data clearly showed that NCp10 favors PSI dimer formation over a broad range of temperatures whereas the D_{tot} values obtained in the absence of NCp10 described a sigmoid curve whose midpoint was around 35 °C (Girard et al., 1995). These results suggest that NCp10 lowers the energy barrier separating the alternative conformations of the C^{278}−G^{303} stem−loop, thus generating a dimerizable conformation of the monomer. In this latter case, the transition is perhaps around 4 °C.

DISCUSSION

A Model of PSI Dimer Formation in Vitro. We previously showed that dimer formation of RNA transcripts derived from the 5′-terminal noncoding region of MoMuLV RNA genome involves a short autocomplementary sequence spanning nucleotides C^{283}−G^{298} in 100 mM NaCl (Girard et al., 1995). We then proposed a three-step mechanism based on this sequence that takes into account (1) a conformational rearrangement of the stem−loop C^{278}−G^{303} induced by temperature (M → M*), (2) a loop−loop recognition (M* + M* ↔ D1), and (3) the reassociation of each stem to generate a stable dimer (D1 → D2). Kinetics of dimerization undertaken at 50 °C should involve only the second and third steps insofar as all RNA molecules are under a dimerizable conformation (M*) at this temperature. With respect to the PSI RNA transcript (nts 215−565), if self-annealing of the C^{278}−G^{303} sequence was solely implicated in dimer formation, we might assume that disruption of this interaction either at low or high ionic strength would lead to an inhibition of dimer formation. On the other hand, if other parts of the RNA transcript were involved in the dimerization through less stable interactions, then increasing the ionic strength would favor these interactions, leading to a salt concentration-dependent dimer formation. Along this line, f215−364 dimer formation is inhibited at 100 mM NaCl (Girard et al., 1995), at 250 mM NaCl, and up to 700 mM NaCl (Figure 2 and data not shown, respectively) by an antisense oligonucleotide complementary to nts 275−291. The same oligonucleotide inhibits f215−565 dimerization at 100 mM (Girard et al., 1995) but not at 250 mM NaCl (Figure 2), indicating that the 364−565 domain could also be involved in PSI dimer formation through intermolecular interactions.

In order to characterize these intermolecular interactions, we have considered the secondary structure of PSI monomer. Tounekti et al. (1992), using chemical probes in solution, showed that PSI is a highly structured domain containing three major subdomains: subdomain 1 (nts 237−381), 2 (nts 382−437), and 3 (nts 438−565) characterized by 5, 2, and 3 stem−loop structures, respectively. We took into account this proposed secondary structure for analyzing the base composition of loops between nts 365 and 565 (see Table 1). Since L1 is complementary to L4 (between nucleotides 5′ G387UUUU 3′ and 3′ C495AAAA) and L2 to L5 (between nucleotides 5′ U416CCCGA and 3′ A535GGGUU), we propose that these short intermolecular Watson−Crick base pairings could cause a transient PSI RNA dimer that favors 5′ U288AGCUA293 3′ loop−loop annealing (Figure 8a). The opening of each stem−loop C^{278}−G^{303} followed by annealing of the autocomplementary sequences C^{283}−G^{298} leads to a more stable dimer. We also propose that

Table 1: Nucleotide Composition of Loops (Denoted L1 to L5) of Subdomains 2 and 3 Derived from the Proposed Secondary Structure of the PSI Monomer Determined in Solution through Chemical Probing (Tounekti et al., 1992)[a]

	subdomain 2	subdomain 3
sequence (from 5′ to 3′)	5′ G^{387}UUUUUGU^{394} 3′ (L1) 5′ A^{415}UCCCGAUCG^{424} 3′ (L2)	5′ U^{451}AGA^{454} 3′ (L3) 5′ C^{489}UAAAACA^{496} 3′ (L4) 5′ U^{529}UUGGGA^{535} 3′ (L5)

[a] Note that L1 is partly complementary to L4 and L2 to L5.

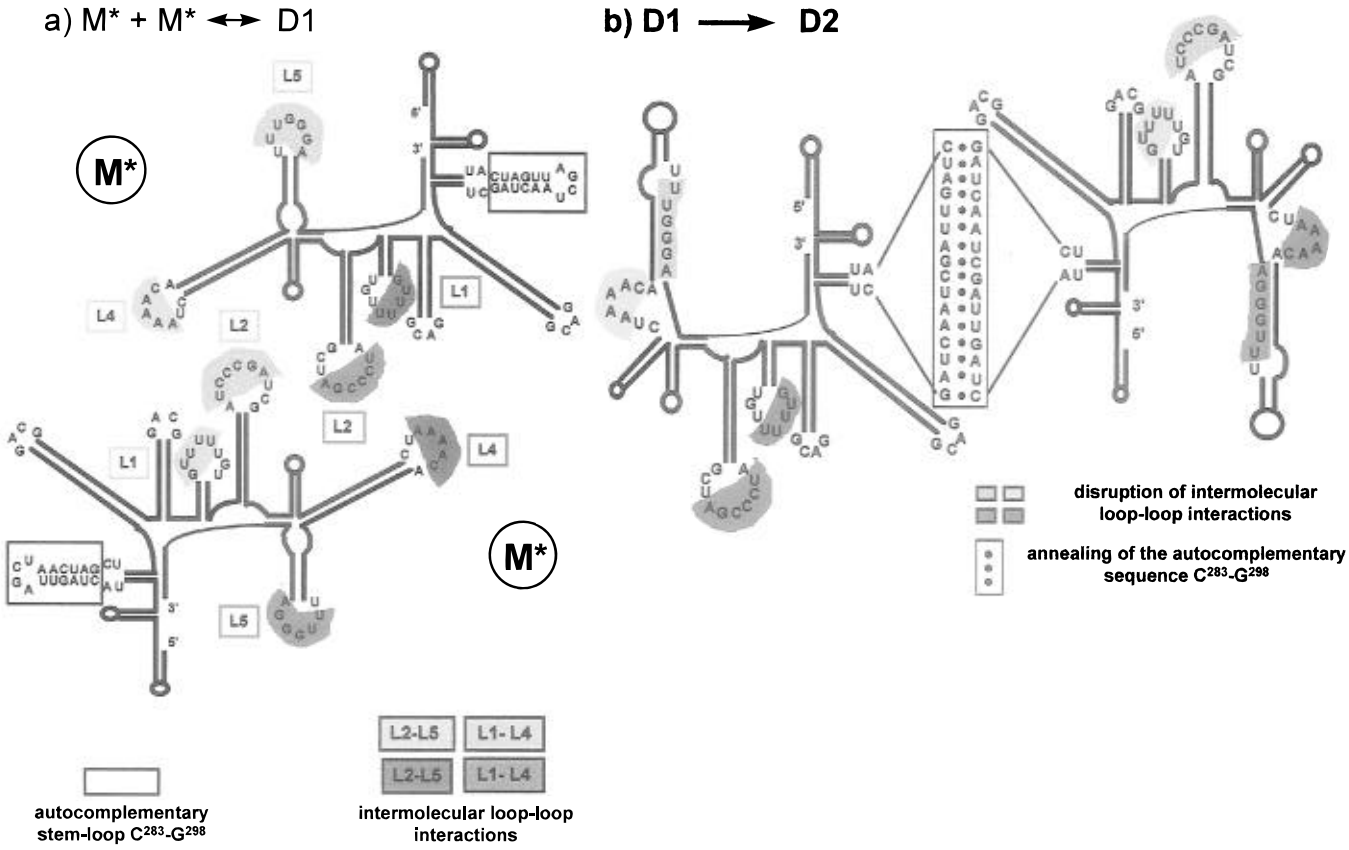

FIGURE 8: Proposed model of PSI dimerization. A transient RNA dimer involving L1−L4 and L2−L5 interactions (a) evolves toward a more stable conformation through the $C^{283}-G^{298}$ autocomplementary sequence (b). M* correspond to dimerizable conformations of monomeric RNA. This model of interaction was drawn by taking into account the proposed monomeric and dimeric secondary structure of PSI determined in solution by chemical probes (Tounekti et al., 1992) and the computer predicted secondary structure using PCFOLD 4.0 [as described previously by Girard et al. (1995)]. Only structural features that are mainly involved in the interaction are pointed out in shading. Bold lines characterize the RNA structural secondary motifs such as loops, bulges, and stem-loops.

this conformational rearrangement changes the conformation of loops L4 and L5, as previously suggested (Tounekti et al., 1992), leading to disruption of the L1−L4 and L2−L5 RNA duplex (Figure 8b).

We made the assumption that, at ionic strength lower than 200 mM NaCl, the L1−L4 and L2−L5 intermolecular interactions are unstable. By increasing the salt concentration up to 300−400 mM NaCl, such intermolecular interactions are stabilized and consequently, the rate constant of PSI dimer formation is increased approximatively 25-fold between 50 and 250 mM NaCl (Figure 3). For salt concentration higher than 300−400 mM NaCl, we suggest that the rate constant decreases due to intramolecular interactions that could compete with intermolecular interactions. Such effect has been already described by Studier (1969), who suggested that an intramolecular restructuration of each single-stranded DNA molecule of T7 phage is unfavorable to double-stranded DNA renaturation while the salt concentration increases. One major point of our system is that when the $G^{279}-U^{302}$ sequence was deleted (such as in f215−565Δ279−302), L1−L4 and L2−L5 intermolecular interactions favored a "transient RNA dimer" that cannot evolve toward a more stable one. When the 364−565 region was deleted together with nts 279−302 (leading to f215−364Δ279−302), D_{tot} and k_1 strongly decreased. This model of dimerization (Figure 8) is in good accordance with the proposed secondary structure of the PSI monomer and dimer (Tounekti et al., 1992) and with the fact that thermal stability of f215−565 (PSI) and f215−364 dimers increased as a function of salt concentration in a similar fashion (Girard et al., 1995).

Another parameter also supports this model. The rate constant k_1 for RNA and DNA duplex formation is connected to [Na+] by the relation $k_1 \approx [Na^+]^{Q/2\xi}$ (thus $\log [k_1] \approx Q/2\xi \log [Na^+]$), where Q is the number of phosphate groups lined up in the initial nonbonded complex and ξ is a dimensionless charge-density parameter [for more details, see Williams et al. (1989) and references therein)]. d log $[k_1]$/d log$[Na^+]$ values determined in our experimental conditions (i.e., between 50 and 350 mM NaCl for f215−565 and f215−565Δ279−302 and between 50 and 700 mM NaCl for f215−364) are reported in Table 2. f215−364Δ279−302 was not considered insofar as this fragment has neither the $C^{278}-$

Table 2: Variation of Rate Constant (k_1) as a Function of Salt Concentration [Na^+]

	d log [k_1]/d log [Na^+][a]	Q[b]
f215−565	2.2 ± 0.4	9 ± 2
f215−565Δ279−302	2.8 ± 0.2	11 ± 2
f215−364	0.9 ± 0.2	4 ± 1

[a] These values were derived from linear regression of the plots of log [k_1] versus log [Na^+] shown in Figure 3b. Only values ranging from 50 to 400 mM NaCl were considered. [b] Q, the number of phosphate groups lined up in the initial nonbonded complex, was calculated using equations derived by Manning [for details see Williams et al., (1989)].

G^{303} stem−loop nor the 364−565 domain. Taking into account that (1) a $Q/2\xi$ value of 3.6 corresponds to 15 nucleotides or phosphate groups in each strand aligned before the first base pair is formed (Williams et al., 1989, and references therein), (2) the transient RNA dimer is the same with regard to f215−565 and f215−565Δ279−302 and is due to L1−L4 and L2−L5 interactions (as postulated), and (3) the transient f215−364 RNA dimer involves only the $U^{288}AGCUA^{293}$ loop, then the maximum Q value for f215−565 and f215−565Δ279−302 is 11 and 6 for f215−364. The measured Q values of 9 ± 2 for f215−565, 11 ± 2 for f215−565Δ279−302, and 4 ± 1 for f215−364 are consistent with this prediction.

The C^{283}−G^{298} Autocomplementary Sequence Is Responsible for RNA Dimer Formation Induced by NCp10. MoMuLV nucleocapsid protein NCp10 is a 56 amino acid polypeptide that contains one CCHC box (Henderson et al., 1981). It has been previously shown that NCp10 highly favors RNA dimer formation *in vitro* (Prats et al., 1988, 1990, 1991). The *in vitro* PSI dimer formation triggered by chemically synthesized NCp10 allowed us to determine the annealing activity of NCp10 in low ionic strength (20 mM Tris-HCl, pH 7.5, 50 mM NaCl, 0.2 mM $MgCl_2$ and 5 mM DTT). The major structural feature involved in PSI dimer formation with NCp10 is also the sequence C^{278}−G^{303} insofar as a deletion of this sequence results in low RNA dimer formation irrespective of NCp10 concentration (Figure 4). Note that k_1 values of f215−565Δ279−302 were greater than those observed for f215−565 at r values < 30, suggesting that deletion of a key dimerization signal apparently results in a combination of faster dimerization kinetics (such as loop−loop interactions) and lower dimerization yield (unstable dimer due to weak interactions). These results are in good agreement with those obtained at low ionic strength without NCp10 [see above and Girard et al. (1995)] and could be explained by the deletion of a sequence-specific binding of NCp10 and/or of the dimer linkage structure of MoMuLV PSI RNA. Such specific binding of HIV-1 nucleocapsid protein (NCp7) to stem−loop structures of HIV-1 PSI RNA has been shown (Sakaguchi et al., 1993; Berkowitz & Goff, 1994; Dannul et al., 1994), but it is unknown if this exists for MoMuLV RNA. Moreover, we observed that the 215−565 RNA dimer formed in the presence of NCp10 is slightly more stable than the one formed without the protein (Figure 7). This indicates that NCp10 could also participate in dimer stabilization by favoring intermolecular interactions.

Our results also show an NCp10 annealing activity over a wide range of Ncp10/RNA molecular ratios (from 10 to 150) as well (i.e., 38−2.5 nts per NCp10) (Figures 4 and 6) with an optimal r value of 40−45 leading to a 10−20-fold

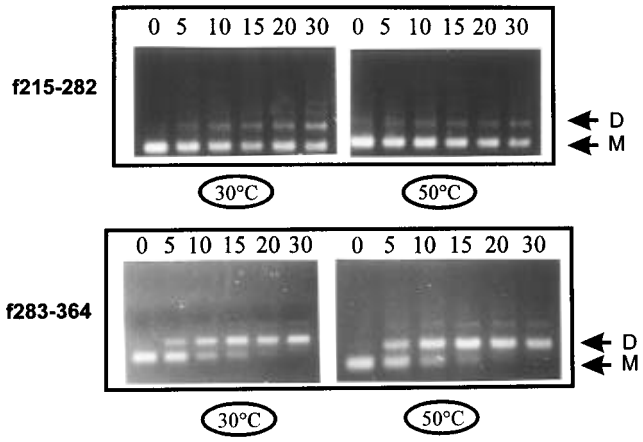

FIGURE 9: Agarose gel electrophoresis of f215−282 and f283−364 dimerization at 30 and 50 °C in the presence of NCp10/RNA molecular ratios (r) between 0 and 30 (i.e., until ≈2−3 nts per NCp10) after an incubation time of 15 min. Experimental conditions were the same as described in Figure 6.

enhancement of PSI dimer formation (Figure 5). Assuming that each protein interacts with the RNA transcripts and has an annealing activity, then these latter values suggest a binding site size of 9 ± 1 nucleotides per NCp10. This value appears to be slightly higher than those already published for several retroviral nucleocapsid proteins: 6 ± 1nts for murine nucleocapsid (NCp10) (Karpel et al., 1987; Casas-Finet et al., 1988; Roberts et al., 1989), 5 ± 1 nts for avian nucleocapsid (NCp12) (Karpel et al., 1987; Jentoft et al., 1988), and 7 ± 1 nts for human nucleocapsid protein (NCp7) (You & McHenry, 1993; Khan & Giedroc, 1994). However, given that part of the RNA is hybridized and, conceivably, that there may still be some internal secondary structures, not all the RNA may be accessible to NCp for binding. Thus, the NCp might bind only to single-stranded regions at equilibrium. This would have the effect of increasing the apparent site size.

NCp10 Destabilizes the C^{278}−G^{303} Stem−Loop. Kinetics of PSI dimer formation performed at temperatures ranging from 4 to 20 °C allowed us to document the annealing activity of NCp10 *in vitro*. At low ionic strength conditions, PSI dimer formation is a slow process that depends on the incubation temperature (Girard et al., 1995). In this study, we showed that NCp10 induces efficient PSI dimerization even at 4 °C (Figure 6), suggesting a strong destabilization of stem−loop structure C^{278}−G^{303} (with a ΔT_M > 30 °C). Note that the non-MoMuLV sequence present at the 5′ end of these transcripts can adopt a stem−loop structure similar to the stem−loop C^{278}−G^{303} (Figure 1). Thus, taking into account a hypothetical loop−loop interaction around the U^8−G^{13} sequence and the opening of each stem, this should lead to the formation of a short RNA duplex. However, as previously reported (Girard et al., 1995), this sequence is not involved in the process of dimerization since f215−282 did not give rise to dimer formation even for a NCp10/RNA molecular ratio of 30, which corresponds to approximatively 2.6 nts per NCp10 (Figure 9). Similar experiments conducted *in vitro* with f283−364, which is also characterized by a stem−loop structure at its 5′ end comprising the C^{283}−G^{298} sequence (Figure 1), showed that for a NCp10/RNA molecular ratio of 10 (i.e., 8−9 nts per NCp10) these transcripts are mainly dimeric at 30 °C (Figure 9). Furthermore, in the absence of NCp10, f283−364 dimer formation was observed at low ionic strength for temperatures >40

Table 3: Comparison between the Free Energy of the Three Stem−Loops [$\Delta G°_{37°C}$(SL)] Shown in Figure 1 and of the Resulting Loop−Loop Interaction [$\Delta G°_{37°C}$(LL)]

sequence	$\Delta G°_{37°C}$(SL)[c] (kcal/mol)	$\Delta G°_{37°C}$(LL) (kcal/mol)	$2\Delta G°_{37°C}$(SL)/ $\Delta G°_{37°C}$(LL)
$G^{1}-C^{20}$	−9.0	−2.6	6.9
GGGCG$C^{283}-G^{298}$	−6.7[a]	−5.2[a]	2.6[a]
	−7.9[b]	−3[b]	5.3[b]
$C^{278}-G^{303}$	−2.6[a]	−5.2[a]	1[a]
	−3.8[b]	−3[b]	2.5[a]

[a] When considering a six-base loop (UAGCUA) (see Figure 1) [b] When considering a four-base loop (AGCU) (see Figure 1). *c* $\Delta G°_{37°C}$(SL) was determined using MFOLD software (Zuker, 1989a,b) and $\Delta G°_{37°C}$(LL) according to the free energy parameters for predictions of RNA duplex stability determined by Freier et al. (1986).

°C (data not shown) whereas 50% of f215−565 dimerization yield took place at 25 °C [see Figure 5 in Girard et al. (1995)]. We then made the assumption that both the free energies of the stem−loop and of the loop−loop interaction are two thermodynamic parameters that could control dimer formation triggered or not by NCp10 *in vitro* (Table 3). Note that Bertrand and Rossi (1994) suggested that, at 37 °C and under physiological salt conditions, NCp7 is able to melt helices rapidly, this melting being dependent upon helix stability rather than helix length.

Darlix and co-workers described an efficient annealing activity of HIV-1 NCp7 for temperatures ranging from 23 to 55 °C in low ionic strength (Lapadat-Tapolsky et al., 1995). NCp10 annealing activity observed between 4 and 20 °C could be considered as being at variance with this report. Assuming that annealing activity is common to retroviral NCp and does not depend on DNA and/or RNA sequence (Khan & Giedroc, 1992; Dib-Hajj et al., 1993; Tsuchihachi et al., 1993; Tsuchihachi & Brown, 1994; Herschlag et al., 1994; Lapadat-Tapolsksy et al., 1995), this discrepancy may be interpreted rather as the result of a temperature-dependent rate constant. From the results reported in this study, we suggest that NCp annealing activity below 30 °C or above 30 °C should be studied after at least a 60 min or a 15 min incubation time, respectively, in order to reach equilibrium.

RNA Dimer Formation in Vivo. This study and a previous one (Girard et al., 1995) showed that destabilization of the $C^{278}-G^{303}$ stem−loop is a key step in RNA dimer formation triggered or not by the NCp10. It is also suggested that an increase in salt concentration favors loop−loop interactions within the 387−535 region. How relevant are these effects *in vivo*? Rein and co-workers have shown that dimeric viral RNA of MoMuLV and HIV-1 undergo a maturation event (from "unstable" to "stable" RNA dimer) after release of the virus from the cell (Fu & Rein, 1993; Fu et al., 1994). Considering the fluctuations of salt concentration inside the cell, which could play a role in the control of nucleic acid-dependent physiological functions (Hardin et al., 1991), we propose that intermolecular loop−loop interactions along the entire MoMuLV RNA genome favor an unstable transient RNA dimer in the nascent viral particle. Moreover, the transition from unstable to stable viral RNA dimer is dependent upon the activity of the viral protease (Fu & Rein, 1993; Fu et al., 1994; Feng et al., 1995) that cleaves the *gag* precursor polyproteins (Kaplan & Swanstrom, 1991; Burstein et al., 1992; Kaplan et al., 1994) leading to a mature NCp in the virion core. We suggest that, due to annealing and unwinding activities of NCp, maturation of viral RNA dimer should correspond to a great extent to the annealing of the autocomplementary sequence identified in human and murine viral strains (Skripkin et al., 1994; Laughrea & Jetté, 1994, 1996; Muriaux et al., 1995; Girard et al., 1995). We also suggest that individual contribution of other intermolecular interactions to dimer stability is weak whereas the sum of these interactions could explain the less thermostable dimer extracted from newly released viral particles.

REFERENCES

Allain, B., Lapadat-Tapolsky, M., Berlioz, C., & Darlix, J.-L. (1994) *EMBO J. 13*, 973−981.

Aronoff, R., Hajjar, A. M., & Linial, M. L. (1993) *J. Virol. 67*, 178−188.

Barany, G., & Merrifield, R. B. (1979) *in The Peptides* (Gross, E., & Meienhofer, J., Eds.), Vol. 2, pp 1−284, Academic Press, New York.

Barat, C., Lullien, V., Schatz, O., Keith, G., Nugeyre, M. T., Grüninger-Leitch, F., Barré-Sinoussi, F., Le Grice, S. F. J., & Darlix, J.-L. (1989) *EMBO J. 8*, 3279−3285.

Barat, C., Schatz, O., Le Grice, S., & Darlix, J.-L. (1993) *J. Mol. Biol. 231*, 185−190.

Bender, W., & Davidson, N. (1976) *Cell 7*, 595−607.

Bender, W., Chien, Y.-H., Chattopadhyay, S., Vogt, P. K., Gardner, M. R., & Davidson, N. (1978) *J. Virol. 25*, 888−896.

Berkowitz, R. D., & Goff, S. P. (1994) *Virology 202*, 233−246.

Bertrand, E. L., & Rossi, J. J. (1994) *EMBO J. 13*, 2904−2912.

Bieth, E., Gabus, C., & Darlix, J.-L. (1990) *Nucleic Acids Res. 18*, 119−127.

Bowles, N. E., Damay, P., & Spahr, P.-F. (1993) *J. Virol. 67*, 623−631.

Burstein, H., Bizud, D., Kotler, M., Schatz, G., Vogt, V. M., & Skalka, A. M. (1992) *J. Virol. 66*, 1781−1785.

Casas-Finet, J. R., Jhon, N. I., & Maki, A. H. (1988) *Biochemistry 27*, 1172−1178.

Cornille, F., Mely, Y., Ficheux, D., Savignol, I., Gerard, D., Darlix, J.-L., Fournié-Zaluski, M.-C., & Roques, B.-P. (1990) *Int. J. Pept. Res. 36*, 551−558.

Covey, S. N. (1986) *Nucleic Acids Res. 14*, 623−633.

Dannull, J., Surovoy, A., Jung, G., & Moelling, K. (1994) *EMBO J. 13*, 1525−1533.

Darlix, J.-L., & Spahr, P.-F. (1982) *J. Mol. Biol. 160*, 147−161.

Darlix, J.-L., Gabus, C., Nugeyre, M.-T., Clavel, F., & Barré-Sinoussi, F. (1990) *J. Mol. Biol. 216*, 689−699.

Darlix, J.-L., Gabus, C., & Allain, B. (1992) *J. Virol. 66*, 7245−7252.

Déméné, H., Jullian, N., Morellet, N., de Rocquigny, H., Cornille, F., Maigret, B., & Roques, B.-P. (1994a) *J. Biomol. NMR 4*, 153−170.

Déméné, H., Dong, C. Z., Ottmann, M., Rouyez, M.-C., Jullian, N., Morellet, N., Mely, Y., Darlix, J.-L., Fournié-Zaluski, M. C., Saragosti, S., & Roques, B.-P. (1994b) *Biochemistry 33*, 11707−11716.

de Rocquigny, H., Gabus, C., Vincent, A., Fournie-Zaluski, M.-C., Roques, B.-P., & Darlix, J.-L. (1992) *Proc. Natl. Acad. Sci. U.S.A. 89*, 6472−6476.

de Rocquigny, H., Ficheux, D., Gabus, C., Allain, B., Fournié-Zaluski, M.-C., Darlix, J.-L., & Roques, B.-P. (1993) *Nucleic Acids Res. 21*, 823−829.

Dib-Hajj, F., Khan, R., & Giedroc, D. P. (1993) *Protein Sci. 2*, 231−243.

Dorfman, T., Luban, J., Goff, S. P., Haseltine, W. A., & Göttlinger, H. G. (1993) *J. Virol. 67*, 6159−6169.

Feng, Y.-X., Fu, W., Winter, A. J., Levin, J. G., & Rein, A. (1995) *J. Virol. 69*, 2486−2490.

Fleissner, E., & Tress, E. (1973) *J. Virol. 12*, 1612−1615.

Freier, S. M., Kierzek, R., Jaeger, J. A., Sugimoto, N., Caruthers, M. H., Neilson, T., & Turner, D. H. (1986) *Proc. Natl. Acad. Sci. U.S.A. 83*, 9373−9377.

Fu, W., & Rein, A. (1993) *J. Virol. 67*, 5443−5449.

Fu, W., Gorelick, R. J., & Rein, A. (1994) *J. Virol. 68*, 5013−5018.

Girard, P.-M., Bonnet-Mathonière, B., Muriaux, D., & Paoletti, J. (1995) *Biochemistry 34*, 9785−9794.

Gorelick, R. J., Henderson, L. E., Hanser, J. P., & Rein, A. (1988) *Proc. Natl. Acad. Sci. U.S.A. 85*, 8420−8424.
Gorelick, R. J., Nigida, S. M., Bess, J. R., Arthur, L. O., Henderson, L. E., & Rein, A. (1990) *J. Virol. 64*, 3207−3211.
Hardin, C. C., Henderson, E., Watson, T., & Prosser, J. K. (1991) *Biochemistry 30*, 4460-4472.
Herschlag, D., Khosla, M., Tsuchihachi, Z., & Karpel, R. L. (1994) *EMBO J. 13*, 2913−2924.
Hu, S., Davidson, N., & Verma, I. M. (1977) *Cell 10*, 469−477.
Jentoft, J. E., Smith, L. M., Fu, X., Johnson, M., & Leis, J. (1988) *Proc. Natl. Acad. Sci. U.S.A. 85*, 7094−7098.
Kaplan, A. H., & Swanstrom, R. (1991) *Proc. Natl. Acad. Sci. U.S.A. 88*, 4528−4532.
Kaplan, A. H., Manchester, M., & Swanstrom, R. (1994) *J. Virol. 68*, 6782−6786.
Karpel, R. L., Henderson, L. E., & Oroszlan, S. (1987) *J. Biol. Chem. 262*, 4961−4967
Khan, R., & Giedroc, D. P. (1994) *J. Biol. Chem. 269*, 22538−22546.
Lapadat-Tapolsky, M., De Rocquigny, H., Van Gent, D., Roques, B., Plasterk, R., & Darlix, J.-L. (1993) *Nucleic Acids Res. 21*, 831−839.
Lapadat-Tapolsky, M., Pernelle, C., Borie, C., & Darlix, J.-L. (1995) *Nucleic Acids Res. 23*, 2434−2441.
Laughrea, M., & Jetté, L. (1994) *Biochemistry 33*, 13464−13474.
Laughrea, M., & Jetté, L. (1996) *Biochemistry 35*, 1589−1598.
Leis, J., Baltimore, D., Bishop, J. M., Coffin, J., Fleissner, E., Goff, S. P., Oroszlan, S., Robinson, H., Skalka, A. M., Temin, H. M., & Vogt, V. (1988) *J. Virol. 62*, 1808−1809.
Long, C. W., Henderson, L. E., & Oroszlan, S. (1980) *Virology 104*, 491−496.
Maisel, J., Bender, W., Hu, S., Duesberg, P. H., & Davidson, N. (1978) *J. Virol. 25*, 384−394.
Mann, R., & Baltimore, D. (1985) *J. Virol. 54*, 401−407.
Mann, R., Mulligan, R. C., & Baltimore, D. (1983) *Cell 33*, 153−159.
Maurer, B., Bannert, H., Darai, G., & Flügel, R. M. (1988) *J. Virol. 63*, 1558−1568.
Mély, Y., Cornille, F., Fournié-Zaluski, M.-C., Darlix, J.-L., Roques, B.-P., & Gerard, D. (1991) *Biopolymers 31*, 899−906.
Méric, C., & Spahr, P.-F. (1986) *J. Virol. 60*, 450−459.
Méric, C., Gouilloud, E., & Spahr, P.-F. (1988) *J. Virol. 62*, 3328−3333.
Morellet, N., Jullian, N., de Rocquigny, H., Maigret, B., Darlix, J.-L., & Roques, B.-P. (1992) *EMBO J. 11*, 3059−3065.
Morellet, N., de Rocquigny, H., Mély, Y., Jullian, N., Déméné, H., Ottmann, M., Gérard, D., Darlix, J.-L., Fournié-Zaluski, M.-C., & Roques, B.-P. (1994) *J. Mol. Biol. 235*, 287−301.
Muriaux, D., Girard, P.-M., Bonnet-Mathonière, B., & Paoletti, J. (1995) *J. Biol. Chem. 270*, 8209−8216.
Murti, K. G., Bondurant, M., & Tereba, A. (1981) *J. Virol. 37*, 411−419.
Nissen-Meyer, J., & Abraham, A. K. (1980) *J. Mol. Biol. 142*, 19−28.
Omichinski, J. G., Clore, G. M., Sakaguchi, K., Appella, E., & Gronenborn, A. M. (1991) *FEBS Lett. 292*, 25−30.
Prats, A.-C., Sarih, L., Gabus, C., Litvak, S., Keith, G., & Darlix, J.-L. (1988) *EMBO J. 7*, 1777−1783.
Prats, A.-C., Roy, C., Wang, P., Erard, D., Housset, V., Gabus, C., Paoletti, C., & Darlix, J.-L. (1990) *J. Virol. 64*, 774−783.
Prats, A.-C., Housset, V., De Billy, G., Cornille, F., Prats, H., Roques, B.-P., & Darlix, J.-L. (1991) *Nucleic Acids Res. 19*, 3533−3541.
Rein, A. (1994) *Arch. Virol. 9*, 513−522.
Rein, A., Harvin, D. P., Mirro, J., Ernst, S. M., & Gorelick, R. J. (1994) *J. Virol. 68*, 6124−6129.
Roberts, W. J., Pan, T., Elliot, J. L., Coleman, J. E., & Williams, K. R. (1989) *Biochemistry 28*, 10043−10047.
Roy, C., Tounekti, N., Mougel, M., Darlix, J.-L., Paoletti, C., Ehresmann, C., Ehresmann, B., & Paoletti, J. (1990) *Nucleic Acids Res. 18*, 7287−7292.
Sakaguchi, K., Zambrano, N., Baldwin, E. T., Shapiro, B. A., Erickson, J. W., Omichinski, J. G., Clore, G. M., Gronenborn, A. M., & Appela, E. (1993) *Proc. Natl. Acad. Sci. U.S.A. 90*, 5219−5223.
Sambrook, J., Fritch, E. F., & Maniatis, T. (1989) *Molecular Cloning: A Laboratory Manual*, 2nd ed., Cold Spring Harbor Laboratory Press, Cold Spring Harbor, NY.
Skripkin, E., Paillart, J.-C., Marquet, R., Ehresmann, B., & Ehresmann, C. (1994) *Proc. Natl. Acad. Sci. U.S.A. 91*, 4945−4949.
Studier, F. W. (1969) *J. Mol. Biol. 41*, 199−209.
Tounekti, N., Mougel, M., Roy, C., Marquet, R., Darlix, J.-L., Paoletti, J., Ehresmann, B., & Ehresmann, C. (1992) *J. Mol. Biol. 223*, 205−223.
Tsuchihachi, Z., & Brown, P. O. (1994) *J. Virol. 68*, 5863−5870.
Tsuchihachi, Z., Khosla, M., & Herschlag, D. (1993) *Science 262*, 99−102.
William, A. P., Longfellow, C. E., Freier, S. M., Kiersek, R., & Turner, D. H. (1989) *Biochemistry 28*, 4283−4291.
You, J. C., & McHenry, C. S. (1993) *J. Biol. Chem. 268*, 16519−16527.
Zuker, M. (1989a) *Methods Enzymol. 180*, 262−303.
Zuker, M. (1989b) *Science 244*, 48−52.

BI952454S